Swapping of the β-Hairpin Region between Sp1 and GLI Zinc Fingers: Significant Role of the β-Hairpin Region in DNA Binding Properties of C_2H_2-type Zinc Finger Peptides†

Yasuhisa Shiraishi, Miki Imanishi, Tatsuya Morisaki, and Yukio Sugiura*

Institute for Chemical Research, Kyoto University, Uji, Kyoto 611-0011, Japan

Received October 15, 2004; Revised Manuscript Received November 24, 2004

ABSTRACT: The recent design strategy of zinc finger peptides has mainly focused on the α-helix region, which plays a direct role in DNA recognition. On the other hand, the study of non-DNA-contacting regions is extremely scarce. By swapping the β-hairpin regions between the Sp1 and GLI zinc fingers, in this study, we investigated how the β-hairpin region of the C_2H_2-type zinc finger peptides contributes to the DNA binding properties. Surprisingly, the Sp1 mutant with the GLI-type β-hairpin had a higher DNA binding affinity than that of the wild-type Sp1. The result of the DNase I footprinting analyses also showed the change in the DNA binding pattern. In contrast, the GLI zinc finger completely lost DNA binding ability as a result of exchanging the β-hairpin region. These results strongly indicate that the β-hairpin region appears to function as a scaffold and has an important effect on the DNA binding properties of the C_2H_2-type zinc finger peptides.

The construction of an artificial DNA binding domain with a specificity for all of the DNA sequences is the powerful tool for gene therapy. Of the DNA binding domains, a C_2H_2-type zinc finger protein has the most potential as a molecule for engineering DNA binders with various sequences because of the following features: (i) a C_2H_2-type zinc finger forms a compact ββα structure by the tetrahedral coodination of the zinc ion using the conserved two cysteines and histidines, (ii) the zinc finger motif exists as the tandemly linked forms, and (iii) each domain generally interacts with three base pairs by the specific positions of the α-helix (*1*−*3*). Therefore, it is possible that the long and nonpalindrome sequences are recognized by the artificial multi-zinc finger proteins. Since the elegant crystal analysis of the Zif268 zinc finger−DNA complex (*4*, *5*), rational (*6*−*11*) and phage display-based designs (*12*−*16*) have been conducted in the α-helix regions based on the Zif268 and Zif268-like zinc fingers. As a result, many DNA recognition codes have been established. However, complicated problems still remain for the completion of the tailor-made zinc fingers. For example, (i) some sequences cannot be specifically recognized (*15*, *16*), and (ii) multi-zinc finger proteins consisting of more than three zinc finger domains do not gain the expected specificity and affinity in proportion to the number of zinc finger domains (*17*, *18*).

The study of the framework of a C_2H_2-type zinc finger is necessary for overcoming these limitations because knowledge of the regions besides the DNA recognition helix is significantly lacking. In recent years, several studies on the connection regions between two zinc finger domains provided useful information for resolving these problems (*19*−*21*). In our opinion, the β-hairpin region not only stabilizes the zinc finger domain, but also contributes to the DNA binding specificity by its interaction with phosphates.

Therefore, we evaluated the effect of the β-hairpin region of the C_2H_2-type zinc finger peptide on the DNA binding properties. In this study, the Sp1 and GLI zinc fingers were selected because both zinc fingers show distinct base and phosphate interactions, and structural and functional information is abundant (*21*−*26*). Sp1 zinc finger, which is a DNA binding domain of the human transcription factor Sp1 extracted from HeLa cells, has three contiguous C_2H_2-type zinc finger domains like the Zif268 zinc finger (*22*−*24*). In particular, the C-terminal two fingers, Sp1(zf23),[1] show the typical three-base-pair recognition mode. On the other hand, the crystal structure of the GLI zinc finger−DNA complex revealed that the C-terminal two zinc fingers of GLI recognize the extensive 10 base pair and also make unusual contacts to phosphates in the β-hairpin region (*25*, *26*). Our previous experiments confirmed that only the C-terminal two fingers, GLI(zf45), bind to the target site with a high affinity (*21*). For the purpose of elucidating the effect of the β-hairpin regions, we designed and compared the β-hairpin swapped mutants between Sp1(zf23) and GLI(zf45). As a result, significant changes in the DNA binding affinity and specificity were found.

MATERIALS AND METHODS

Chemicals. The T4 polynucleotide kinase and restriction enzymes were purchased from New England Biolabs. The

* To whom correspondence should be addressed. Phone: +81-774-38-3210. Fax: +81-774-32-3038. E-mail: sugiura@scl.kyoto-u.ac.jp.

† This study was supported in part by Grants-in-Aid for COE Project "Element Science" (12CE2005) and Scientific Research (16659028·14370755) from the Ministry of Education, Culture, Sports, Science, and Technology, Japan. Y.S. is a research fellow of the Japan Society for the Promotion of Science.

[1] Abbreviations: Tris, tris(hydroxymethyl)aminomethane; TN, Tris-NaCl; CD, circular dichroism; zf, zinc finger.

10.1021/bi047797h CCC: $30.25
Published on Web 01/22/2005

Taq DNA polymerase and synthesized oligonucleotides for cloning each peptide were acquired from Qiagen and SIGMA GENOSYS, respectively. The labeled [γ-^{32}P] ATP compound was supplied by DuPont. The plasmid pBS-Sp1-fl was kindly provided by Dr. R. Tjian. All other chemicals were of commercial reagent grade.

Preparations of Zinc Finger Peptides and Substrate DNA Fragments. Sp1(zf23), Sp1(zf123), and GLI(zf45) are coded on the plasmids pEVSp1(530−623), pEVSp1(566−623), and pEVGLI(99−160), respectively, as previously described (*21*). The other mutants were constructed using the standard PCR technique with Sp1(zf23) and GLI(zf45) as templates. Their sequences were confirmed by a GeneRapid DNA sequencer (Amersham Biosciences). These zinc finger peptides were overexpressed as a soluble form in the *Escherichia coli* strain BL21(DE3)pLysS at 25 °C and purified according to the previous procedure at 4 °C (*21*), except that 1 mM PMSF was added at the step of resuspending and lysing in GLI-(zf45) and GLI(zf45)BG. The substrate DNAs in this experiment (GC box and GLIseq) were prepared as in a previous experiment (*21*). The *Hin*d III−*Xba* I fragments (GC box: 41 bp and GLIseq: 50 bp, respectively) were cut out and labeled at the 5′-end with ^{32}P for the previously described experiments (*7*).

CD Measurements. The CD spectra for all the zinc finger peptides were recorded on a Jasco J-720 spectropolarimeter using a 0.10-cm path length quartz cell at 20 °C. The CD spectra are averages of 10 scans, collected at 0.5-nm intervals between 200 and 280 nm. All the CD samples were diluted to obtain 10 μM of the zinc finger peptide in 10 mM Tris-HCl (pH 8.0), 50 mM NaCl, and 1 mM dithiothreitol.

Gel Mobility Shift Assays. Gel mobility shift assays were carried out under the previous experimental conditions (*27*). Each reaction mixture contained 10 mM Tris-HCl (pH 8.0), 50 mM NaCl, 1 mM dithiothreitol, 10 μM $ZnCl_2$, 25 ng/μL poly(dI-dC), 0.05% Nonidet P-40, 5% glycerol, 40 μg/mL bovine serum albumin, the ^{32}P-end-labeled substrate DNA fragment (∼50 pM, 500 cpm), and 0−4 μM of the zinc finger peptide. After incubation at 20 °C for 30 min, the sample was run on an 8% polyacrylamide gel with 89 mM Tris-borate buffer at 20 °C. The bands were visualized by autoradiography and quantified with ImageMaster 1D Elite software (version 3.01). The dissociation constants (K_d) of the Sp1 and GLI peptide−DNA fragment complexes were estimated according to a previously reported procedure (*28*).

DNase I Footprinting Analyses. DNase I footprinting experiments were performed according to the method of Brenowitz et al. (*29*). The binding mixture contained 10 mM Tris-HCl (pH 8.0), 50 mM NaCl, 25 ng/μL poly(dI-dC), 0.05% Nonidet P-40, 40 μg/mL bovine serum albumin, 5 mM $CaCl_2$, 10 mM $MgCl_2$, the 5′-end-labeled substrate DNA fragment (∼6 nM, 30 Kcpm), and 0−4 μM peptide. According to the previous procedure, the following steps were accomplished (*21*).

Methylation Interference Analyses. The recognition of guanines in the primary and secondary strands of the GC box (the G- and the C-strands, respectively) by each peptide was investigated by methylation interference assays as previously described (*30*). The binding reaction mixture contained 10 mM Tris-HCl (pH 8.0), 50 mM NaCl, 1 mM dithiothreitol, 10 μM $ZnCl_2$, 25 ng/μL poly(dI-dC), 0.05% Nonidet P-40, 5% glycerol, 40 μg/mL bovine serum albumin, the ^{32}P-end-labeled methylated DNA fragment (∼60 nM, 500 Kcpm), and 20−500 nM of the zinc finger peptide. The reaction and analysis steps were the same as the previous conditions (*21*).

RESULTS

Designs of Zinc Finger Peptides and Substrate DNAs. The base recognition mode of the Sp1 zinc finger (*28*) is shown in Figure 1A. Figure 1B shows the recognition mode of GLI-(zf45) determined by an X-ray structural analysis (*26*). Sp1-(zf23)BG and GLI(zf45)BS were prepared by exchanging the β-hairpin regions between Sp1(zf23) and GLI(zf45) (Figure 1C). For comparison to the wild-type Sp1 zinc finger Sp1(zf123), Sp1(zf123)BG was also constructed by adding the finger 1 region to Sp1(zf23)BG. As for the substrate DNAs, the GC box for the Sp1-type mutants and GLIseq for GLI-type mutants were used as in the previous experiment (*21*).

CD Spectral Features of Zinc Finger Peptides. The information about the secondary structure of each peptide was checked by measurements of the CD spectra. The CD features of the peptides at 20 °C are presented in Figure 2. The CD characteristics for Sp1(zf23) and GLI(zf45) were similar to those from the previous experiment (*21*). In general, the CD spectrum of a C_2H_2-type zinc finger peptide shows the negative Cotton effects in the far-UV region with a minimum around 208 nm and a shoulder around 222 nm. Both Sp1(zf23)BG and GLI(zf45)BS formed the expected structures of the C_2H_2-type zinc finger peptides as a result of the β-hairpin swapping. The values at 222 nm of GLI-(zf45) ($[\theta] = -7714$) and GLI(zf45)BS ($[\theta] = -9403$) were greater than those of Sp1(zf23) ($[\theta] = -3029$) and Sp1-(zf23)BG ($[\theta] = -3084$), respectively, suggesting a structural difference in the histidine−histidine spacing (*21*, *31*). Furthermore, one unique difference was observed at around 208 nm. The values of the mutants with the GLI-type β-hairpin region, Sp1(zf23)BG ($[\theta] = -5175$) and GLI(zf45) ($[\theta] = -8501$), were smaller than those of the mutants with the Sp1-type β-hairpin region, Sp1(zf23) ($[\theta] = -8234$) and GLI(zf45)BS ($[\theta] = -12886$), respectively, reflecting the subtle structural change in the β-hairpin region.

DNA Binding Affinity of Each Zinc Finger Peptide. To evaluate the effect of the β-hairpin region on the DNA binding affinity, we performed the gel mobility shift assays. Figure 3 shows the representative data, and the determined apparent dissociation constants (K_d) are listed in Table 1. The values of Sp1(zf123), Sp1(zf23), and GLI(zf45) are cited from the previous result (*21*). The binding affinity of Sp1-(zf123)BG ($K_d = 1.0$ nM) was 13-fold higher than that of Sp1(zf123) (K_d=13 nM), while only a subtle change was detected between the K_d value of Sp1(zf23) for the GC box (340 nM) and that of Sp1(zf23)BG (720 nM). For the GLI-type peptide, in contrast, GLI(zf45)BS completely lost the DNA binding ability for GLIseq despite the existence of the recognition helix. These results provide interesting evidence for the role of the β-hairpin regions in DNA binding of the C_2H_2-type zinc finger peptides.

DNA Binding Modes of Zinc Finger Peptides Detected by Footprinting Technique. To determine the DNA binding mode of the Sp1-type mutants, DNase I footprinting was applied. The data from the DNase I footprinting analyses

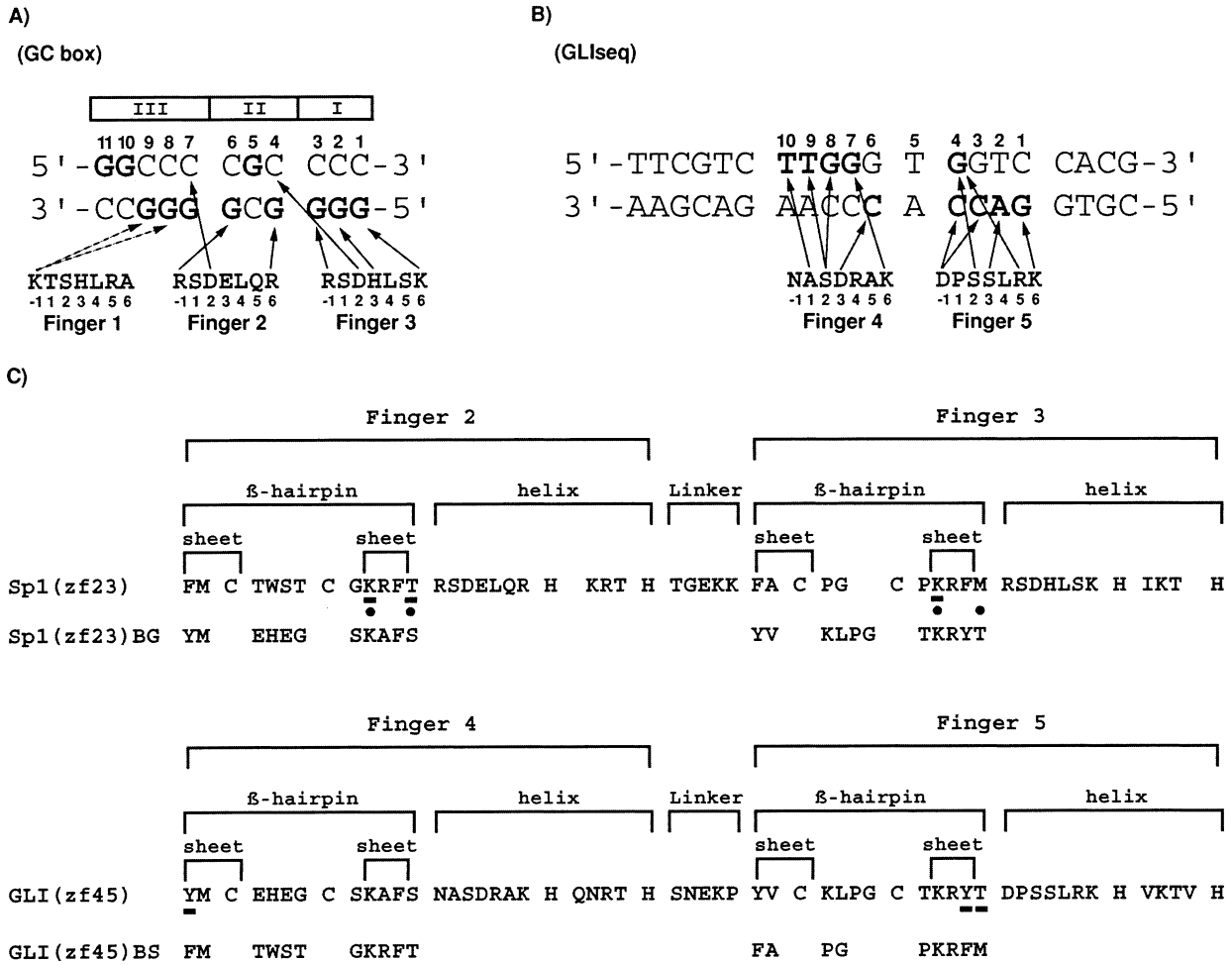

FIGURE 1: (A) Putative base recognition mode of three zinc fingers of Sp1. Amino acid residues at the N-terminus of the α-helix in each finger are depicted by their one-letter codes with the number of the helical positions below. Solid arrows show the amino acid−base interactions based on the DNA binding mode of Zif268, and the dotted arrows depict the contacts indicated by our previous report (*28*). The guanine bases, whose methylation interferes with the zinc finger binding, are in bold print. GC box is divided into three subsites (subsites I, II, and III) for convenience. (B) DNA recognition mode of the C-terminal two zinc fingers of GLI determined by X-ray crystal structure (*26*). Solid arrows show the base recognition, and the bases recognized by amino acids are written in bold characters. (C) Primary structures of two-finger-type zinc finger peptides. The designation of each zinc finger is shown by the original name. The amino acid residues of each peptide are indicated by their one-letter codes. Solid lines under Sp1(zf23) and GLI(zf45) present the residues that make phosphate contacts in the β-hairpin regions, and the positions of the phosphate contacts observed in the Zif268 zinc finger are indicated by solid circles.

for the G-strand are shown in Figure 4, and the hypersensitive cleavages by DNase I were labeled (a) to (d) depending on their positions. Sp1(zf23) exhibited an extended footpinting pattern including subsite III, as shown in the previous result (*28*). The hypersensitive cleavages (a) and (b) in and near subsite III were observed, but the footprint in subsites I and II of Sp1(zf23)BG was not very evident. In the three-finger-type mutants of Sp1, both Sp1(zf123) and Sp1(zf123)BG protected the GC box region, but the positions of the hypersensitive cleavages were changed. Sp1(zf123) presented two hypersensitive cleavages (c) and (d). On the other hand, the hypersensitive cleavages (b) appeared in Sp1(zf123)BG and the hypersensitive cleavage (d) of Sp1(zf123)BG was weaker than that of Sp1(zf123). These results suggest that the DNA binding mode of the Sp1-type mutants is evidently affected by the substitution of the β-hairpin regions.

Evaluation of Sequence-Specific DNA Recognition Mode of Sp1-type Zinc Fingers. Methylation interference analyses are available for detecting the guanine base recognition; therefore, we performed the methylation interference analyses for the bindings of Sp1(zf123) and Sp1(zf123)BG to the GC box (Figure 5). Unfortunately, the Sp1(zf23)BG result was not obtained due to the low DNA binding affinity of Sp1(zf23)BG. Sp1(zf123) made contact with all of the guanines at positions 1−12, although the recognition level was weak only at G7 (Figure 5, lanes 3, 4, 9, and 10) (*21*). The recognition pattern of Sp1(zf123)BG was almost the same as Sp1(zf123) in both the G- and C-strands, including the unique five-guanine base recognition mode of finger 1. From these results, presumably, the enhanced DNA binding affinity and the distinct footprint pattern of Sp1(zf123)BG are not caused by the change in the base recognition mode.

DISCUSSION

To date, more than 10 different types of β-turns have been identified and classified. Each β-turn distinctly affects the local β-sheet properties, such as the hydrogen-bond register, β-sheet twist, and β-sheet stability (*32*−*34*). In C_2H_2-type zinc fingers, several different β-turns exist depending on the number and sequence of amino acids between the two ligand cysteines (*35*). Sp1(zf23) has type II and type I β-turns in fingers 2 and 3, respectively. On the other hand, GLI(zf45)

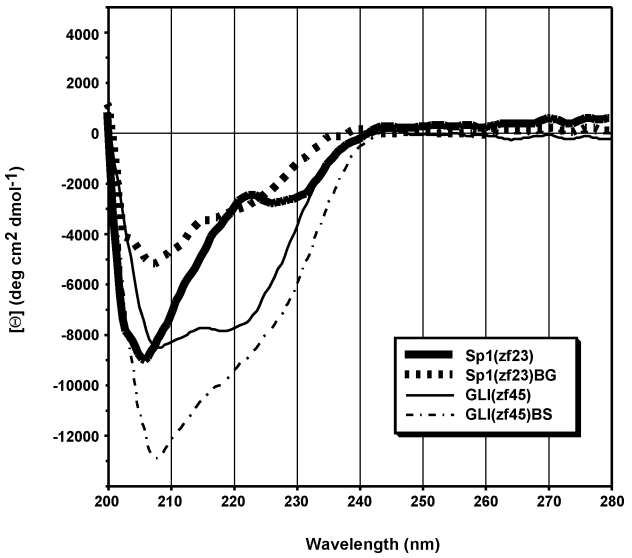

FIGURE 2: CD spectra of two-finger-type zinc finger peptides of Sp1 and GLI at 20 °C. Sp1(zf23), Sp1(zf23)BG, GLI(zf45), and GLI(zf45)BS are indicated by a bold solid line, bold dashed line, solid line, and dashed line, respectively.

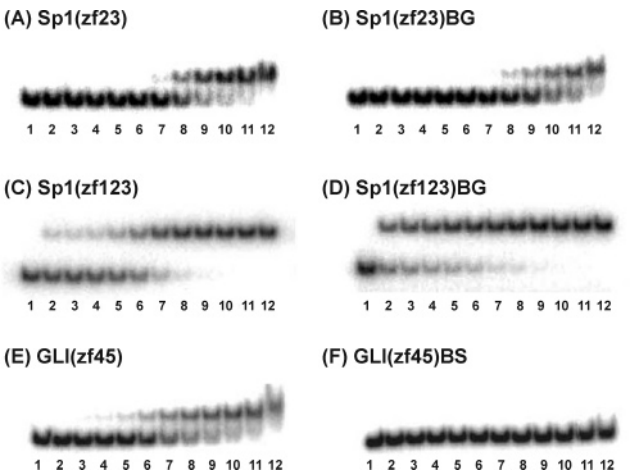

FIGURE 3: Gel mobility shift assays for Sp1(zf23), Sp1(zf23)BG, Sp1(zf123), and Sp1 (zf123)BG binding to GC box, respectively (A−D), and for GLI(zf45) and GLI(zf45)BS binding to GLIseq (E and F). In panels A, B, E, and F, lanes 1−12 contain 0, 3.9, 7.8, 15.6, 31.3, 62.5, 125, 250, 500, 1000, 2000, and 4000 nM peptide, respectively. In panels C and D, lanes 1−12 contain 0, 0.5, 1, 2, 3.9, 7.8, 15.6, 31.3, 62.5, 125, 250, and 500 nM peptide, respectively.

forms type IV and type II β-turns in fingers 4 and 5, respectively (*24*, *26*). In our CD spectral results, the difference between the mutants with the Sp1-type β-hairpin and with the GLI-type β-hairpin was evidently observed at around 208 nm. From a previous report, the β-turns yield various curve shapes that correlate with the β-turn types, although these turn spectra have relatively small ellipticities compared with those of the α-helix and β-sheet (*34*). Therefore, the alteration of spectral patterns may reflect the structural difference of β-hairpin region depending on β-turn types.

The gel mobility shift assays exhibit a drastic change in the DNA binding affinity in both the Sp1-type and GLI-type mutants. The framework of the Sp1 zinc finger has a structure typical of the Zif268 zinc finger, and then successful rational and selection-based designs based on the Sp1 framework have been conducted (*6*−*9*, *11*, *15*, *16*). On the basis of these facts, the structures of the Sp1 and Zif268 zinc finger seem to be the most sophisticated and suitable motif. However, the DNA binding affinity of Sp1(zf123)-BG is increased about one order over that of Sp1(zf123). The result reveals that zinc fingers in nature still have room for improving the DNA binding ability. Furthermore, GLI-(zf45)BS showed no DNA binding for GLIseq, despite the fact that the α-helix region and linker region, which play a significant role in DNA binding, are unchanged. SNEKP linker of GLI(zf45) has flexible conformation, and the DNA binding affinity for GLIseq is hardly affected by exchanging of the histidine spacing from HX_4H to HX_3H (*21*, *36*). Therefore, our previous proposal that the unique extensive DNA recognition mode of GLI(zf45) is sustained by the character of each zinc finger domain is strongly supported by the present result.

To clarify the relationship between the increase in the DNA binding affinity and the alteration of the DNA binding mode, DNase I footprinting analyses were performed. The hypersensitive cleavage appears at the 3′ site of the binding region, in the specific binding of C_2H_2-type zinc finger to the target site (*21*, *27*). The distinct footprint patterns were detected between Sp1(zf23) and Sp1(zf23)BG, although these DNA binding affinities were nearly the same. Sp1(zf23) protected the overall GC box region including subsite III and also showed no hypersensitive cleavage found in the previous experiment (*28*). This observation suggests that Sp1-(zf23) has a low specificity for subsites I and II. On the other hand, Sp1(zf23)BG produced a hypersensitive cleavage around subsite III and the weak footprint in subsites I and II, indicating that Sp1(zf23)BG binds more specifically to subsites I and II, as compared with Sp1(zf23). In addition, a different footprinting pattern was detected between Sp1-(zf123) and Sp1(zf123)BG. The hypersensitive cleavages (c) and (d) were induced by Sp1(zf123) (*27*, *28*). In Sp1(zf123)-BG, both of these cleavages were also detected. However, the strength of cleavage (d) was evidently weakened instead of the appearance of cleavage (b). The hypersensitive cleavage (b) was also observed in Sp1(zf23)BG. On the other hand, the position of cleavage (b) was protected in Sp1-(zf123). In our opinion, the DNA binding mode of Sp1-(zf123)BG for the GC box is optimized because of the specific binding of the Sp1(zf23)BG region, leading to the enhancement of the DNA binding affinity. Furthermore, the base recognition mode between Sp1(zf123) and Sp1(zf123)-BG was compared using the methylation interference technique. Despite the significant difference in the DNA binding affinity and DNA binding mode, the base recognition pattern was identical to each other. This result indicates that the base−amino acid interactions are hardly affected by the structural change in the β-hairpin region.

In general, the C_2H_2-type zinc fingers can be divided into two types of DNA binding modes, i.e., Zif268-type and non-Zif268-type. In the Zif268-type zinc fingers, continuous domains are connected by a highly conserved TGEKP linker that forms a stable structure upon DNA binding and optimizes the zinc finger−DNA orientation for the three-base-pair recognition mode (*3*, *36*). On the other hand, the non-Zif268-type zinc fingers hold flexible linkers with various lengths, and hence, each domain has a unique DNA binding mode (*26*, *37*, *38*). It is still unclear how the DNA binding mode of the non-Zif268-type zinc fingers is deter-

Table 1: Apparent Dissociation Constants (K_d) for Spl(zf23), Spl(zf23)BG, Spl(zfl23), and Spl(zf123)BG Bindings to GC Box and for GLI(zf45) and GLI(zf45)BS Bindings to GLIseq

	K_d (nM)[a]					
binding site[b]	Spl(zf23)	Spl(zf23)BG	Spl(zfl23)	Spl(zfl23)BG	GLI(zf45)	GLI(zf45)BS
GC box	3.4 ($\pm$0.2) $\times$ 10^2	7.2 ($\pm$0.7) $\times$ 10^2	1.3 ($\pm$0.1) $\times$ 10	1.0 $\pm$ 0.2		
GLIseq					3.8 ($\pm$0.3) $\times$ 10^2	NB[c]

[a] Apparent dissociation constants were determined by titration using a gel mobility shift assay as described in Materials and Methods. Values are averages of three or more independent determinations with standard deviations. [b] The nomenclature is described in the text (see Figure 1). [c] NB denotes not binding.

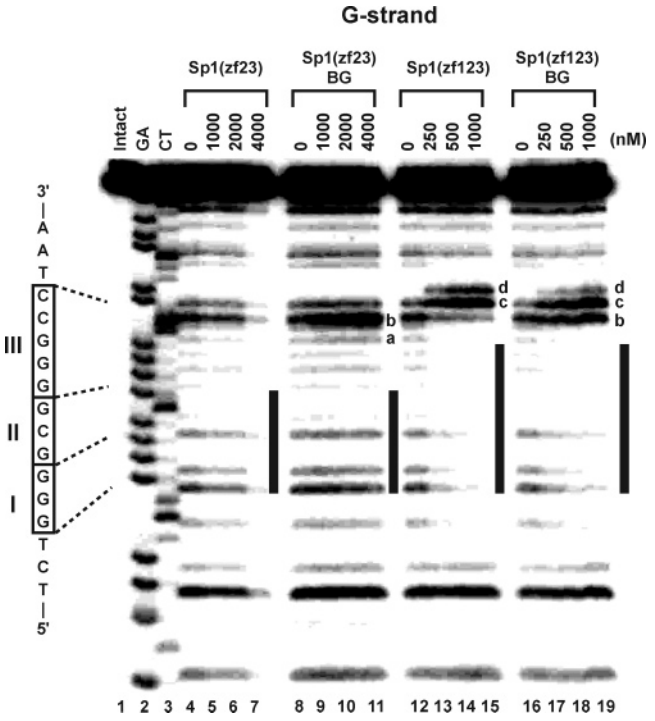

FIGURE 4: DNase I footprinting analyses of Sp1(zf23), Sp1(zf23)-BG, Sp1(123), and Sp1(123)BG bindings to the GC box. This panel shows the results for the G strand of the GC box. The characters (a) through (d) represent the enhanced sites of cleavage caused by the binding of each peptide. Bold bar shows the promising binding site of each peptide. Lane 1, intact DNA; lane 2, G+A (Maxam−Gilbert reaction products); lane 3, C+T (Maxam−Gilbert reaction products). Every peptide concentration is noted in the figure.

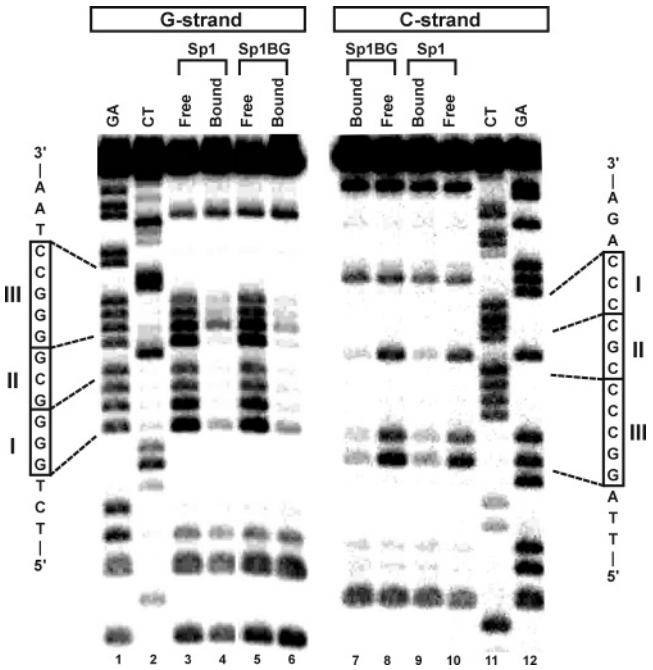

FIGURE 5: Methylation interference analyses of the binding of three-finger-type peptides of Sp1 to the GC box. Sp1 and Sp1BG denote Sp1(zf123) and Sp1(zf123)BG, respectively. The left (lanes 1−6) and right (lanes 7−12) panels show the results for the G- and C-strands, respectively. Lanes 1 and 12, G+A (Maxam−Gilbert reaction products); lanes 2 and 11, C+T (Maxam−Gilbert reaction products); lanes 3, 5, 8, and 10, free DNA samples; lanes 4, 6, 7, and 9, peptide-bound DNA samples.

mined. The complete loss of the DNA binding ability of GLI-(zf45)BS strongly indicates that the β-hairpin region significantly participates in the DNA binding of the non-Zif268-type zinc fingers. In addition to the structural change in the β-hairpin region, the functional effect would be considered by comparison with the Zif268-type zinc fingers. The GLI zinc finger exhibits amino acid−phosphate interaction patterns different from those of the Zif268-type zinc fingers (Figure 1C) (*26*). One interesting fact is that the tyrosine residue occupies the conserved aromatic positions in the β-hairpin region of GLI and makes hydrogen bonds with the phosphate backbone. In contrast, phenylalanine is conserved in the Zif268-type zinc fingers. The same tendency is also observed in other non-Zif268-type zinc fingers such as the TFIIIA and TTK zinc finger (*37*, *38*). In our opinion, therefore, the Zif268-type zinc fingers establish a three-base-pair recognition mode by virtue of the structural characteristic of the TGEKP linker, whereas the non-Zif268-type zinc fingers construct a unique DNA binding mode by making use of various phosphate contacts. The change in the DNA binding mode of the Sp1-type zinc finger would also reflect the distinct orientation for the substrate DNA depending on the change in the phosphate contacts. Of course, further structural analyses using NMR and X-ray must be carried out. Judging from the fact that Sp1(zf123)BG gained a higher DNA binding affinity than the wild-type Sp1, a more precise strategy including the framework is required for the new design of zinc finger proteins.

REFERENCES

1. Fairall, L., Rhodes, D., and Klug, A. (1986) Mapping of the sites of protection on a 5 S RNA gene by the Xenopus transcription factor IIIA. A model for the interaction, *J. Mol. Biol. 192*, 557−591.
2. Frankel, A. D., Berg, J. M., and Pabo, C. O. (1987) Metal-dependent folding of a single zinc finger from transcription factor IIIA, *Proc. Natl. Acad. Sci. U.S.A. 84*, 4841−4845.
3. Wolfe, S. A., Nekludova, L., and Pabo, C. O. (2000) DNA recognition by Cys2His2 zinc finger proteins, *Annu. Rev. Biophys. Biomol. Struct. 29*, 183−212.
4. Pavletich, N. P., and Pabo, C. O. (1991) Zinc finger-DNA recognition: crystal structure of a Zif268-DNA complex at 2.1 Å, *Science 252*, 809−817.
5. Elrod-Erickson, M., Rould, M. A., Nekludova, L., and Pabo, C. O. (1996) Zif268 protein-DNA complex refined at 1.6 Å: a model

system for understanding zinc finger-DNA interactions, *Structure 4*, 1171−1180.
6. Desjarlais, J. R., and Berg, J. M. (1992) Toward rules relating zinc finger protein sequences and DNA binding site preferences, *Proc. Natl. Acad. Sci. U.S.A. 89*, 7345−7349.
7. Desjarlais, J. R., and Berg, J. M. (1992) Redesigning the DNA-binding specificity of a zinc finger protein: a data base-guided approach, *Proteins 12*, 101−104.
8. Desjarlais, J. R., and Berg, J. M. (1992) Redesigning the DNA-binding specificity of a zinc finger protein: a data base-guided approach, *Proteins 13*, 272.
9. Desjarlais, J. R., and Berg, J. M. (1993) Use of a zinc-finger consensus sequence framework and specificity rules to design specific DNA binding proteins, *Proc. Natl. Acad. Sci. U.S.A. 90*, 2256−2260.
10. Sera, T., and Uranga, C. (2002) Rational design of artificial zinc-finger proteins using a nondegenerate recognition code table, *Biochemistry 41*, 7074−7081.
11. Nagaoka, M., Shiraishi, Y., Uno, Y., Nomura, W., and Sugiura, Y. (2002) Interconversion between serine and aspartic acid in the alpha helix of the N-terminal zinc finger of Sp1: implication for general recognition code and for design of novel zinc finger peptide recognizing complementary strand, *Biochemistry 41*, 8819−8825.
12. Choo, Y., and Klug, A. (1994) Toward a code for the interactions of zinc fingers with DNA: selection of randomized fingers displayed on phage, *Proc. Natl. Acad. Sci. U.S.A. 91*, 11163−11167.
13. Choo, Y., and Klug, A. (1994) Selection of DNA binding sites for zinc fingers using rationally randomized DNA reveals coded interactions, *Proc. Natl. Acad. Sci. U.S.A. 91*, 11168−11172.
14. Greisman, H. A., and Pabo, C. O. (1997) A general strategy for selecting high-affinity zinc finger proteins for diverse DNA target sites, *Science 275*, 657−661.
15. Segal, D. J., Dreier, B., Beerli, R. R., and Barbas, C. F., III. (1999) Toward controlling gene expression at will: selection and design of zinc finger domains recognizing each of the 5′-GNN-3′ DNA target sequences, *Proc. Natl. Acad. Sci. U.S.A. 96*, 2758−2763.
16. Dreier, B., Beerli, R. R., Segal, D. J., Flippin, J. D., and Barbas, C. F., III. (2001) Development of zinc finger domains for recognition of the 5′-ANN-3′ family of DNA sequences and their use in the construction of artificial transcription factors, *J. Biol. Chem. 276*, 29466−29478.
17. Kamiuchi, T., Abe, E., Imanishi, M., Kaji, T., Nagaoka, M., and Sugiura, Y. (1998) Artificial nine zinc-finger peptide with 30 base pair binding sites, *Biochemistry 37*, 13827−13834.
18. Nagaoka, M., Kaji, T., Imanishi, M., Hori, Y., Nomura, W., and Sugiura, Y. (2001) Multiconnection of identical zinc finger: implication for DNA binding affinity and unit modulation of the three zinc finger domain, *Biochemistry 40*, 2932−2941.
19. Moore, M., Choo, Y., and Klug, A. (2001) Design of polyzinc finger peptides with structured linkers, *Proc. Natl. Acad. Sci. U.S.A. 98*, 1432−1436.
20. Nomura, W., and Sugiura, Y. (2003) Effects of length and position of an extended linker on sequence-selective DNA recognition of zinc finger peptides, *Biochemistry 42*, 14805−14813.
21. Shiraishi, Y., Imanishi, M., and Sugiura, Y. (2004) Exchange of histidine spacing between Sp1 and GLI zinc fingers: distinct effect of histidine spacing-linker region on DNA binding, *Biochemistry 43*, 6352−6359.
22. Dynan, W. S., and Tjian, R. (1983) Isolation of transcription factors that discriminate between different promoters recognized by RNA polymerase II, *Cell 32*, 669−680.
23. Kadonaga, J. T., Jones, K. A., and Tjian, R. (1986) Promoter-specific activation of RNA polymerase II transcription by Sp1, *Trends Biochem. Sci. 11*, 20−23.
24. Narayan, V. A., Kriwacki, R. W., and Caradonna, J. P. (1997) Structures of zinc finger domains from transcription factor Sp1. Insights into sequence-specific protein-DNA recognition, *J. Biol. Chem. 272*, 7801−7809.
25. Kinzler, K. W., Ruppert, S. H., Bigner, S. H., and Vogelstein, B. (1988) The GLI gene is a member of the Kruppel family of zinc finger proteins, *Nature 332*, 371−374.
26. Pavletich, N. P., and Pabo, C. O. (1993) Crystal structure of a five-finger GLI-DNA complex: new perspectives on zinc fingers, *Science 261*, 1701−1707.
27. Uno, Y., Matsushita, K., Nagaoka, M., and Sugiura, Y. (2001) Finger-positional change in three zinc finger protein Sp1: influence of terminal finger in DNA recognition, *Biochemistry 40*, 1787−1795.
28. Yokono, M., Saegusa, N., Matsushita, K., and Sugiura, Y. (1998) Unique DNA binding mode of the N-terminal zinc finger of transcription factor Sp1, *Biochemistry 37*, 6824−6832.
29. Brenowitz, M., Senear, D. F., Shea, M. A., and Ackers, G. K. (1986) Quantitative DNase footprint titration: a method for studying protein-DNA interactions, *Methods Enzymol. 130*, 132−181.
30. Wissmann, A., and Hillen, W. (1991) DNA contacts probed by modification protection and interference studies, *Methods Enzymol. 208*, 365−379.
31. Kochoyan, M., Keutmann, H. T., and Weiss, M. A. (1991) Alternating zinc fingers in the human male-associated protein ZFY: HX3H and HX4H motifs encode a local structural switch, *Biochemistry 30*, 9396−9402.
32. Lewis, P. N., Momany, F. A., and Scherage, H. A. (1973) Chain reversals in proteins, *Biochim. Biophys. Acta 303*, 211−229.
33. Richardson, J. S. (1981) The anatomy and taxonomy of protein structure, *Adv. Protein Chem. 34*, 167−339.
34. Rose, G. D., Gierasch, L. M., and Smith, J. A. (1985) Turns in peptides and proteins, *Adv. Protein Chem. 37*, 1−109.
35. Viles, J. H., Patel, S. U., Mitchell, J. B., Moody, C. M., Justice, D. E., Uppenbrink, J., Doyle, P. M., Harris, C. J., Sadler, P. J., and Thornton, J. M. (1998) Design, synthesis and structure of a zinc finger with an artificial beta-turn, *J. Mol. Biol. 279*, 973−986.
36. Laity, J. H., Dyson, H. J., and Wright, P. E. (2000) DNA-induced alpha-helix capping in conserved linker sequences is a determinant of binding affinity in Cys(2)-His(2) zinc fingers, *J. Mol. Biol. 295*, 719−727.
37. Fairall, L., Schwabe, J. W., Chapman, L., Finch, J. T., and Rhodes, D. (1993) The crystal structure of a two zinc-finger peptide reveals an extension to the rules for zinc-finger/DNA recognition, *Nature 366*, 483−487.
38. Nolte, R. T., Conlin, R. M., Harrison, S. C., and Brown, R. S. (1998) Differing roles for zinc fingers in DNA recognition: structure of a six-finger transcription factor IIIA complex, *Proc. Natl. Acad. Sci. U.S.A. 95*, 2938−2943.

BI047797H